On synchronization in power-grids modelled as networks of second-order Kuramoto oscillators

J. M. V. Grzybowski, E. E. N. Macau, and T. Yoneyama

Articles you may be interested in

On synchronization in power-grids modelled as networks of second-order Kuramoto oscillators

J. M. V. Grzybowski,[1] E. E. N. Macau,[2] and T. Yoneyama[3]

[1]*UFFS—Federal University of Fronteira Sul, Rodovia RS 135 km 72, CEP 99.700-000 Erechim, Rio Grande do Sul, Brazil*
[2]*INPE—National Institute for Space Research, Av. dos Astronautas, 1758, Jd. Granja, CEP 12.227-010 São José dos Campos, Sao Paulo, Brazil*
[3]*ITA—Aeronautics Institute of Technology, Pça Marechal Eduardo Gomes, 50, Vila das Acácias, CEP 12.228-615 São José dos Campos, Sao Paulo, Brazil*

This work concerns analytical results on the role of coupling strength in the phenomenon of onset of complete frequency locking in power-grids modelled as a network of second-order Kuramoto oscillators. Those results allow estimation of the coupling strength for the onset of complete frequency locking and to assess the features of network and oscillators that favor synchronization. The analytical results are evaluated using an order parameter defined as the normalized sum of absolute values of phase deviations of the oscillators over time. The investigation of the frequency synchronization within the subsets of the parameter space involved in the synchronization problem is also carried out. It is shown that the analytical results are in good agreement with those observed in the numerical simulations. In order to illustrate the methodology, a case study is presented, involving the Brazilian high-voltage transmission system under a load peak condition to study the effect of load on the syncronizability of the grid. The results show that both the load and the centralized generation might have concurred to the 2014 blackout. *Published by AIP Publishing.*
[http://dx.doi.org/10.1063/1.4967850]

Power-grids are recognized as the largest man-made machines and their proper functioning relies heavily on the synchronization and balance of the interconnected devices. Understanding the conditions under which synchronization can be lost allows us to conceive the grid in such a manner so as to prevent them. The study of power-grid models can enhance such comprehension and provide insights to make them more robust and reliable. In this study, an analytical expression is provided to estimate the coupling strength for the onset of complete frequency locking in networks of second-order Kuramoto oscillators. Good matching is obtained when the analytical results are compared to the experimental outcomes obtained by numerical simulations. As a case study, the proposed estimation method is applied to the Brazilian Interconnected power system, in order to evaluate how synchronization might have been hampered by the concurrence of heavy power transfer and centralized generation in the 2014 blackout.

I. INTRODUCTION

Power grids are large scale distributed dynamical systems with a functional structure involving a number of subsystems. Usually, they consist of a large number of heterogeneous components that operate interconnected, forming a complex network structure. In this network, the interconnected nodes can either perform an energy supplier role or an energy consumer one. Furthermore, the role of a specific node can change over time. The proper functioning of a power grid requires an appropriate management of the power generation so that in an

integrated way they are able to sustain and satisfy the energy demands (loads) of the consumers[23,24] at any given time. In order to accomplish this, it is necessary to be able to deal with episodes of unexpected changes in the load demand by the consumers, with eventual failure of the energy generating units and with disruptions of the transmission lines. In this context, frequency synchronization is an essential feature in alternating current (AC) systems. The matched timing of injection of electrical torques in the network allows for constructive interference of the power injected by each generator in the grid, thus increasing the power available to be transferred to loads. Whenever a generator goes beyond a very narrow tolerable margin of frequency mismatch in relation to the rest of the grid, it must be disconnected from the grid in order to avoid voltage fluctuations or even physical damage to the generator. Such disconnection causes redistribution of power flow in the system, which in turn may lead to problems to generation/load balance, overloads, load shedding, and further contingencies.

These disturbances may lead to the occurrence of local instabilities, which may propagate as a cascade wave through the power grid network. As this process evolves, the cascading disruptions may lead to blackouts ranging from local, short-lived unavailability to full system collapse lasting for several hours or even days. Take as examples the large blackouts in North America and Italy, both in (2003), whose major causes included the inability of the power-grids to regain operational stability after power flow redistributions triggered by the tripping of transmission lines shorted to ground.[1,7,16,17] A more recent example of a large-scale event was the 2014 blackout in Brazil reportedly due to a short

circuit of a key high-voltage line which happened to be running under heavy power transfer regime across the country at the time of failure.[30]

Therefore, power grid systems must be designed to be resilient to local instabilities,[34] failures,[9,35,38] and disturbances.[15,18,40] The stability and robustness of such systems are closely related to the individual characteristics of the oscillators, as well as to the couplings among them reflected in the topology of the network.[2,3,13,25,28,35] Several studies show that valuable insights into the dynamical behavior of power-grids can be gained by means of theoretical studies that consider models of electrical generators coupled according to network structures that reproduce the topological and electrical interactions existing in real power-grids.[3,8–10,15,18,21,28,38] The second-order Kuramoto oscillators are used in Ref. 15 to describe the dynamics of coupled rotating machines, generators, and motors. In Refs. 3–5, 12, 13, and 15, a major object of interest is to investigate the transition from a synchronous state to an incoherent state (or vice-versa) from the viewpoint of complex networks. For instance, it was found in Ref. 25 that, by means of the application of the concept of basin stability,[26,37] nodes adjacent to dead ends or dead trees generally have poorer stability, thus being particularly vulnerable to perturbations.[25] For a detailed review of the state-of-the-art concerning the second-order Kuramoto oscillator, one can mention Ref. 33. It is noteworthy that over the last four decades since it was proposed, the Kuramoto model has been successfully applied in a number of fields ranging from Neuroscience to Earth science,[33] leading to intensive research activities aimed at deepening and sharpening the understanding of its dynamics (see Refs. 11, 14, 19, 22, 27, 29, 39, and 42). A number of studies exists that focus the synchronization and stability issues in the second-order Kuramoto model, such as in Refs. 3–5, 12, 13, 15, 18, 29, 32, and 36. Not only the characterization of the phase transition is of interest but also admissible classes of initial configurations and natural frequency distributions which lead to synchronization.[4] Sufficient conditions for initial setups leading to asymptotic complete phase-frequency synchronization were derived in Ref. 4 on the basis of fixed conditions on inertia, coupling strength, and natural frequencies of the oscillators. The conditions also apply to non-identical oscillators and are tied to requirements on the magnitude of inertia and the diameter of natural frequencies, defined as $D_\Omega(t) = max|\Omega_i - \Omega_j|$, $i, j = 1, \dots, N$, where Ω_i, Ω_j are the natural frequencies of oscillators i, j, respectively. In power-grids, stable asymptotic synchronization is actually directly related with inertia, as synchronous inertia of the system opposes sudden changes in frequency due to disturbances, thus enhancing stability. Similar conclusions using numerical investigations were drawn in Ref. 29. There, for both Gaussian and Lorentzian distributions, the threshold value for the transition from incoherence to coherence states was reported to be dependent on system size and inertia. The authors reported that the hysteresis in the phase transition occurs for large enough inertia. Similar results had been previously reported for damped driven pendula with finite (large) inertia.[41] On the other hand, in Ref. 34, a study based on a second-order Kuramoto model shows that distributed

generation helps decrease the number of crucial links in a network, thus reducing the probability of global failures and facilitating the emergence of complete synchronization. Subsequently, an extended version of the second-order Kuramoto model which takes into account the interplay between voltage and angular stabilities was proposed in Ref. 36. There, voltage stability means the ability of a power system to maintain steady voltages along buses following a disturbance, whereas angle stability addresses the ability of restoring the equilibrium state between input (mechanical torque) and output (electrical torque). It turns out that this extended model allows one to make predictions for a variety of scenarios involving disturbances. Furthermore, the transition to non-stationary states is more feasible due to the existence of a smaller stability region as compared with those obtained with the classical model.[36] Indeed, this extended model can be applied to the study of the dynamical stability of a power system undergoing a short-circuit.

In this paper, the generator/machine model proposed in Ref. 15 is considered, together with the previous studies on the Kuramoto model[3,6,13] to develop analytical expressions for the critical coupling strength associated with the transition from unsynchronized to synchronized state in power grids. The analytical results are then evaluated using an order parameter based on the ideas of partial synchronization presented by Gomez-Gardenes *et al.*[20] The numerical results obtained by evaluating the order parameter over subsets of the synchronization problem are shown to be tight and in good agreement with those obtained from the analytical expressions. The main contribution of the paper is given in Section III, as an explicit algebraic expression for the estimation of the onset of complete frequency locking. It is shown that the diameter of angular frequencies of oscillators plays an important role in the estimation of the critical value for synchronization.

The paper is organized as follows: Section II presents the Kuramoto-like model with bimodal distribution[15] and some results on the critical coupling for synchronization.[3,6,13] Section III develops an estimate for the actual value of the coupling parameter for the onset of complete frequency locking. Section IV presents simulation results. Section V discusses the results and put them in perspective of similar studies in the literature. Finally, Section VI gives final remarks.

II. A MODEL FOR SYNCHRONOUS ELECTRICAL GENERATORS AND LOADS

Consider a network of oscillators with the dynamics given by the second order Kuramoto model, as proposed in Ref. 15. Following Ref. 15, the system equations can be written as

$$\dot{\theta}_j = \omega_j$$
$$\dot{\omega}_j = -\alpha\omega + P_j + P_{max} \sum_{k=1}^{N} A_{jk} \sin(\theta_k - \theta_j) \qquad (1)$$

in which θ_j and ω_j are functions of time and denote the phase and angular velocity of the *j*th oscillator, respectively, α is the damping parameter related to the power dissipation, P_j is

the normalized power delivered by ($P_j > 0$) or consumed by ($P_j < 0$) the jth node, P_{max} is the maximum capacity of the transmission line between two nodes, which corresponds to the coupling strength between two oscillators, and A_{jk} is the entry of the symmetric adjacency matrix at row j and column k that is equal to one if nodes j and k are linked and to zero, otherwise. In the context of power-grids, nodes with $P_i > 0$ are regarded as energy suppliers or generators (G), whereas nodes with $P_i < 0$ are energy consumers or motors (M). In a network of coupled generators and motors, the synchronous state can be taken as $\omega_1(t) = \omega_2(t) = \cdots = \omega_N(t)$, which means that the angular velocities of all the oscillators are equal to the synchronous velocity $\omega_s(t)$, that is, $\dot{\omega}_j - \dot{\omega}_k = 0$. Following Carareto et al.,[3] one takes the condition $\dot{\omega}_j = 0$, $\omega_j = \omega_s$, $j = 1, 2, \ldots, N$ for some constant synchronous angular velocity ω_s, such that Equation (1) becomes

$$0 = -\alpha\omega_s + P_j + P_{max}\sum_{k=1}^{N} A_{jk}\sin(\Delta_{kj}) \quad (2)$$

with $\Delta_{kj} = \theta_k - \theta_j$ a given constant. Under these conditions, it was shown in Ref. 3 that the summation of the equations of the N nodes yields the synchronous angular velocity

$$\omega_s = \sum \frac{P_j}{\alpha N}. \quad (3)$$

In a power-grid, the balance between generators and consumers requires that $\sum_{j=1}^{N} P_j = 0$, which means that $\omega_s = 0$. Over the time, whenever these conditions are not satisfied, instabilities may appear. Two indicators can be used to evaluate how effective a specific power grid is in terms of handling instabilities: *synchronization quality* and *persistence over time*. The former refers to how tight is the matching among the angular velocities of the oscillators, whereas the latter refers to the amount of time they remain synchronized during a sufficiently large time interval. Actually, as time passes, consumer's power request keep changing which requires continuous adjustments in the power supplied by the generators. This, in turn, implies that the synchronous angular velocity keeps changing over the time.

In fact, it can be shown that there is a lower bound for the existence of a synchronous manifold for a network of coupled second-order Kuramoto oscillators, given by[3]

$$P_{sm} = \max_{j}\left\{\frac{|\alpha\omega_s - P_j|}{d_j}\right\}, \quad (4)$$

where $d_j = \sum_{k=1}^{N} A_{jk}$ is the degree of node j.

Based on this lower bound, one can state the following Lemma (see Ref. 3 for demonstration):

Lemma 1. *(Existence of a synchronous manifold[3]). Consider the second-order Kuramoto model given by Eq. (1), with a damping $\alpha > 0$ and coupling strength P_{max}. A necessary condition for frequency synchronization of this system is that*

$$P_{max} \geq P_{sm} \triangleq \max_{j}\left\{\frac{|\alpha\omega_s - P_j|}{d_j}\right\} \quad (5)$$

in which P_j, $j = 1, \ldots, N$ is the power injected/consumed by node j and d_j represents its degree.

This indicates that the variance in the distribution of P_j has to be compensated with stronger coupling or a high value of the node connectivity (node degree). This can also be seen as one examines the coupling strength at the onset of complete frequency locking for a fully connected network.

Consider the deviation equations $\ddot{\theta}_i - \ddot{\theta}_j$ given by

$$\dot{\omega}_i - \dot{\omega}_j = -\alpha(\omega_i - \omega_j) + (P_i - P_j) + P_{max}E(\theta_i, \theta_j, \theta_k) \quad (6)$$

and, as shown by Spong et al.,[6] the maximum value for the function

$$E(\theta_i, \theta_j, \theta_k) = 2\sin(\theta_j - \theta_i)$$
$$+ \sum_{k=1, k\neq i,j}^{N}(\sin(\theta_k - \theta_i) + \sin(\theta_j - \theta_k)) \quad (7)$$

with respect to the phase angles θ_i, θ_j, θ_k, which is achieved for $\theta_i = \theta_j$ or $2\theta_k = \theta_i + \theta_j$. In case $\theta_i = \theta_j$, there is no power flow, and thus, this case is not of interest. For $2\theta_k = \theta_i + \theta_j$, the function 7 reaches a maximum.[6] The coupling function E is related to the intensity of the interplay among a node and its neighbors, and its maximum corresponds to the state of maximum power transfer. The optimal solution $(\theta_j - \theta_i)_{opt}$ gives the maximum of 7 whose value is an explicit function of the number of oscillators for the network, N. As presented in Ref. 6, at the optimal phase difference condition

$$(\theta_j - \theta_i)_{opt} = 2\arccos\left(\frac{-(N-2) + \sqrt{(N-2)^2 + 32}}{8}\right) \quad (8)$$

so that the function 7 yields

$$E_{max} = 2\sin(\theta_j - \theta_i)_{opt} + 2(N-2)\sin\left(\frac{(\theta_j - \theta_i)_{opt}}{2}\right). \quad (9)$$

The behavior of E_{max} as a function of the number of oscillators is depicted in Figure 1. Hence, the Kuramoto model adopted in this work, Eq. (9), leads to a tight lower bound to the onset of complete frequency locking, compatible to that originally presented in Ref. 6 and recently refined in Ref. 13. Following Refs. 6 and 13, this condition for the second-order Kuramoto model can be stated as follows.

Lemma 2. *(Tight critical coupling[6,13]) Consider $(\theta_j - \theta_i)_{opt}$ and E_{max} as in Eqs. (8) and (9), respectively. A necessary condition for frequency synchronization of the second-order Kuramoto model in Eq. (1), $N \geq 2$, and coupling strength P_{max} is that*

$$P_{max} \geq P_{critical} \triangleq \max\frac{|P_i - P_j|}{E_{max}} \quad (10)$$

in which P_i, P_j, i, $j = 1, \ldots, N$ are the generated/consumed power and $(\theta_j - \theta_i)_{opt} \in [\frac{\pi}{2}, \pi]$.

Section III examines the relation between the necessary conditions required in Lemmas 1 and 2. Furthermore, by considering the influence of angular velocities, a way is
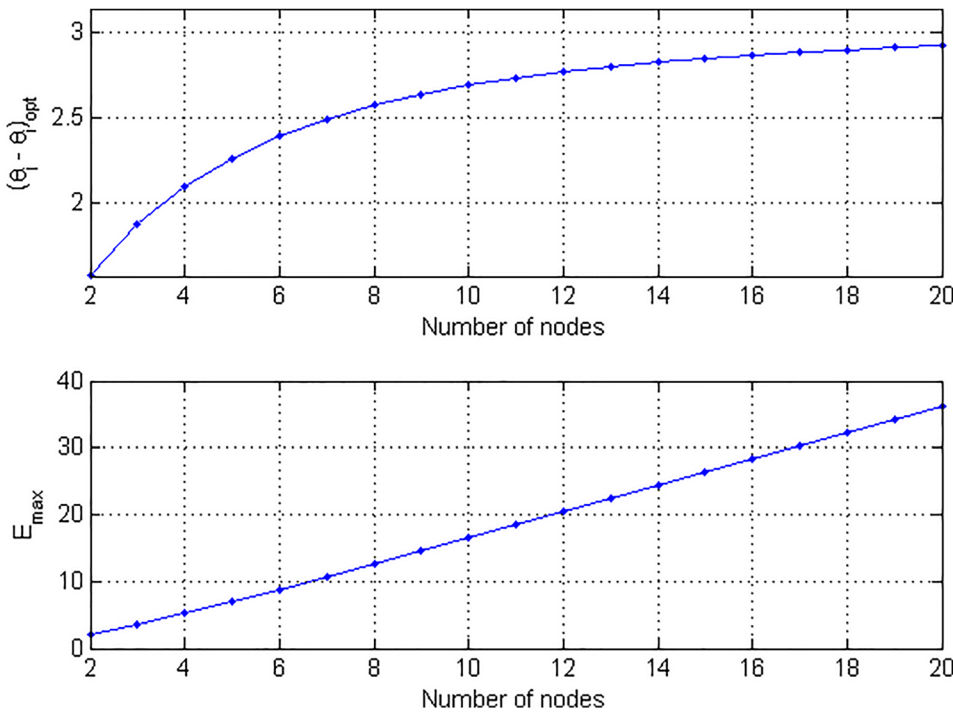
FIG. 1. Evolution of the optimal phase angle $(\theta_j - \theta_i)_{opt}$ as a function of the number of nodes N in the network (above) and evolution of the value of E_{max} as a function of the optimal phase angle and the number of nodes. The value of E_{max} allows us to estimate the value of the minimum coupling value for which synchronization can be achieved.

provided to estimate the actual onset of complete frequency locking for networks of second-order Kuramoto oscillators with all-to-all couplings.

III. COUPLING FOR THE ONSET OF COMPLETE FREQUENCY LOCKING: THE NECESSARY CONDITIONS AND A CLOSER ESTIMATE

As $(\theta_j - \theta_i) \to (\theta_j - \theta_i)_{opt}$ one has $E \to E_{max}$. Now, consider Eq. (8) and assume $E = E_{max}$ for the purpose of finding P_{max} for the onset of complete frequency locking. Also, denote $\omega_i - \omega_j = \Delta\omega_{ij}$ in Eq. (6), yielding the following linear ODE:

$$\Delta\dot{\omega}_{ij} + \alpha\Delta\omega_{ij} = (P_i - P_j) + P_{max}E_{max} \qquad (11)$$

whose solution is given by

$$\Delta\omega_{ij} = \frac{P_i - P_j}{\alpha} + \frac{P_{max}E_{max}}{\alpha} + \Delta\omega_0 e^{-\alpha t} \qquad (12)$$

for some arbitrary integration constant $\Delta\omega_0$. As $t \to +\infty$, the exponential term vanishes and one can rearrange the equation such that

$$P_{max} > max\frac{|\alpha\Delta\omega_{ij} - (P_i - P_j)|}{E_{max}}, \quad i,j = 1,...,N. \qquad (13)$$

Equation (13) provides a lower bound for P_{max} that allows synchronization. Assuming P_i, P_j as constants, one can approximate the value of P_{max} by evaluating the upper bound for the deviation in angular velocities, $\Delta\omega_{max}$. Consider that the angular velocity for a given oscillator will have a value in the interval $[\omega_{min}, \omega_{max}]$, in which $\omega_{min} = min(\omega_i)$ and $\omega_{max} = max(\omega_i)$, $i = 1,...,N$. One can define this interval by observing that for a weak coupling condition, each

oscillator will rotate with angular velocity corresponding to its natural frequency as $t \to +\infty$, that is,

$$\omega_i = \frac{P_i}{\alpha}. \qquad (14)$$

On the other hand, for strong coupling and $t \to +\infty$,

$$\omega_i = \omega_s = \sum_{i}^{N} \frac{P_i}{\alpha N} \qquad (15)$$

so that

$$\Delta\omega_{max} = \omega_{max} - \omega_{min} = max_i \left|\frac{\sum_{i}^{N} P_i - NP_i}{\alpha N}\right|. \qquad (16)$$

Thus, the value of P_{max} from Equation (13) can be estimated for a given network of coupled generators/consumers by the expression

$$P_{max}^{**} = max\left\{\frac{|\alpha\Delta\omega_{max} - (P_i - P_j)|}{E_{max}}\right\}, \quad i,j = 1,...,N. \qquad (17)$$

Note that as ω_i, ω_j eventually evolve to the same value, Equation (6) becomes

$$0 = (P_i - P_j) + P_{max+}2\sin(\theta_j - \theta_i)$$
$$+ \sum_{k=1,k\neq i,j}^{N}(\sin(\theta_j - \theta_k) + \sin(\theta_j - \theta_k)) \qquad (18)$$

and, by different means, one recovers the expression

$$P_{max}^{*} = max\frac{|P_i - P_j|}{E_{max}}, \qquad (19)$$

which is the value below which synchronization between nodes i and j cannot be achieved, as established in Lemma 2. In other words, $P_{max} > P^*_{max}$ is a necessary condition for synchronization. Figure 2 shows the evolution of P^*_{max}, P^{**}_{max}, and P_{SM} as a function of the number of nodes N to networks with all-to-all couplings, $P_i = (-1)^i$, $i = 1, ..., N$. Note that $P^*_{max} \geq P_{SM}$ for all N, which makes P^*_{max} a less strict necessary condition for synchronization when $|P_i| = |P_j|$, $i,j = 1, ..., N$. However, this is not the case if $|P_i| \neq |P_j|$, $i,j = 1, ..., N$ as P^*_{max} gives lower values than P_{sm}. Thus, in all cases, one should choose $max\{P^*_{max}, P_{sm}\}$ as a necessary condition for the onset of complete frequency locking. A more realistic estimation would consider unmatched angular velocities, and in this case, Equation (19) cannot be applied. In such cases, P^{**}_{max} given by Equation (17) provides the amount of power transfer capability that would allow the network to remain synchronous or to regain synchrony after a perturbation.

Another element in making the model dynamics more akin to that of power-grids is by working around the assumption of full connectedness of the corresponding network matrix. Towards that end, consider the network adjacency matrix A which induces the network Laplacian matrix $G = D - A$, where D is a diagonal matrix whose entries are defined as $D_{ii} = \sum_{j=1}^{N} A_{ij}$. Consider the Laplacian matrix G of a highly connected undirected and unweighted network with N nodes, such that λ_2 is its smallest nonzero eigenvalue, also known as the algebraic connectivity of the network. Further, consider a fully connected network with N nodes whose Laplacian matrix is G^{full} and define λ_2^{full} in an analogous manner. As one considers networks of oscillators that are not fully connected, the assumption made for the calculation of E_{max} is not satisfied. In other words, the derivation of an expression for E_{max} relies upon the assumption of a fully connected network. To generalize the result to networks modeled by not fully connected undirected Laplacian matrices, we refer to the work by Carareto *et al.*[3] which established that, for highly connected networks, the scaling

$$P_{max} = \frac{\lambda_2^{full}}{\lambda_2} P_{max}^{full} \tag{20}$$

holds.

In the adopted power-grid model, $\Delta\theta_{jk}(t) = c$ indicates that the phase difference between two oscillators j and k is a constant. In turn, time-varying $\Delta\theta_{jk}(t)$ indicates that frequencies are not matched. Assume, therefore, that one can measure the phase differences $\Delta\theta(t)$ for every pair of oscillators over the network to form a matrix with entries $\Delta\theta_{jk}(t)$. Its mean value over the time can be regarded as a measure of the overall state of network synchronization, and it can be associated with the previous defined overall quality and persistence of synchronization. It follows that the level of coherence in the power-grid model can be accessed by means of a parameter r_f defined as

$$r_f = \frac{1}{N(N-1)} \sum_{k=1}^{N} \sum_{j=1, j\neq k}^{N} \left(\left\| \lim_{\Delta t \to +\infty} \frac{1}{\Delta t} \int_{t_r}^{t_r + \Delta t} e^{i(\theta_j - \theta_k)} dt \right\| \right) \tag{21}$$

in which $r_f \in [0, 1]$, $r_f = 0$ indicates totally incoherent or intermittent states, $r_f = 1$ indicates perfectly matched angular velocities over time, and $r_f \in (0, 1)$ corresponds to intermittent or partial synchronization. This order parameter given by Equation (21) can be calculated within subsets of the parameter space and then presented in the form of coherence
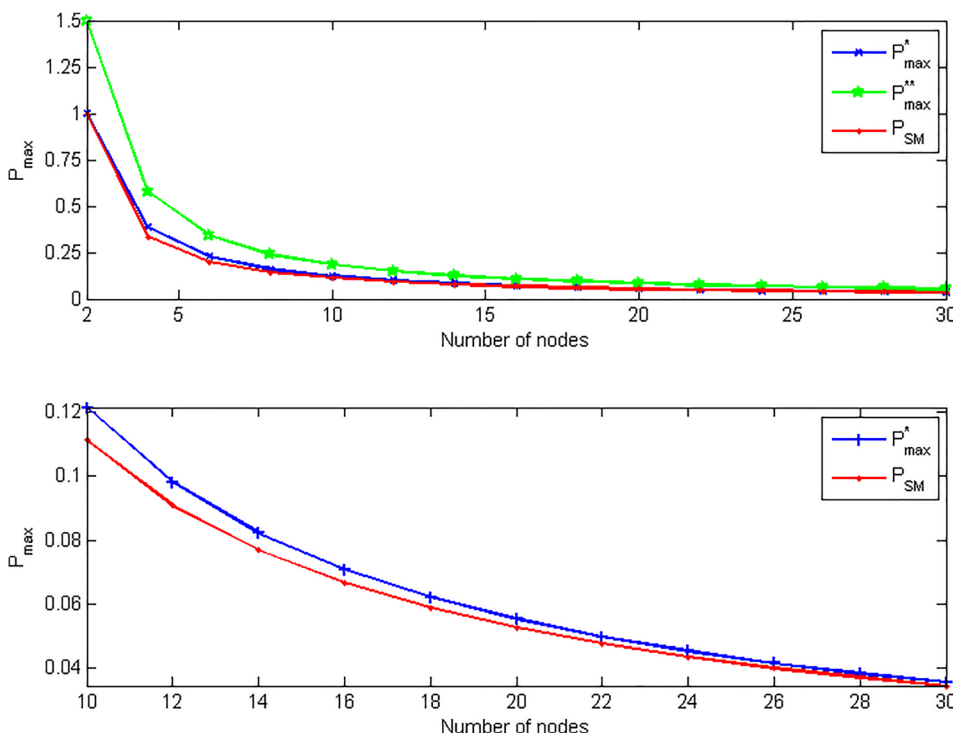

FIG. 2. (a) Evolution of P^*_{max}, P^{**}_{max} and P_{SM} as a function of the number of the nodes N of an all-to-all network. As P^*_{max} and P_{sm} are necessary conditions for synchronization and P^*_{max} is more restrictive in this case, the synchronization can only emerge if $P_{max} \geq P^*_{max}$. A more realistic estimate for the onset of complete frequency locking, as explained above, is given by P^{**}_{max}. (b) A closer look into the evolution of P^*_{max} and P_{sm}.

maps from which the synchronization figure in diverse network structures and parameter subsets can be studied. Section IV explored such plots by means of numerical simulation.

IV. RESULTS

In what follows, the results derived in Section III are compared using numerical simulations. The integration was performed using the 4th order Runge–Kutta algorithm and with a time step $h = 10^{-3}$. Apart from checking the validity of the theoretical results, the numerical simulations shall allow an evaluation of the effects of different levels of distributed generation on the value of the minimal coupling. More specifically, networks with fixed power demand and different sizes are studied. The conditions under which each of the simulations was performed are given in the figure captions. Following Ref. 12, we define γ as the length of the shortest arc in the cycle that covers the geodesic distance between any two initial condition angles of the oscillators. Thus, for example, if $\theta_1 = \pi/4$, $\theta_2 = \pi/3$, and $\theta_3 = \pi/2$, then the shortest arc γ lies in the clockwise subtraction $\gamma = \pi/2 - \pi/4 = \pi/4$. This parameter is used along with coupling strength to study the onset of complete frequency locking.

A. Two nodes: Generator-motor

The numerical simulation shown in Figure 3 illustrates the application of theoretical results in a network of mutually coupled second-order Kuramoto oscillators, which corresponds to the simplest case. The numerical values chosen for this simulation are $P_{max} = 1.5$, $\alpha = 0.2$, $P_1 = 2$, $P_2 = -1$ and initial conditions $(\theta_j - \theta_i)_{opt}$ and $\omega_1 = \omega_2 = 0$. Note that this is the critical coupling value given by Equation (19) for the maintenance of synchronization in the case when all the frequencies are matched. As $\Delta\omega = 0$, Equation (19) holds and the oscillators remain synchronized over time, as shown in Figure 4. On the other hand, a large set of numerical simulations for P_{max} below the threshold showed that synchronization is lost as $t \to +\infty$, which is also the case when $\Delta\omega(0) \neq 0$. Numerical simulations revealed that synchronization is not maintained for $P_{max} < 1.5$, as predicted by theory.

B. Fixed power demand for different network sizes

It can be noticed from the theoretical results and numerical simulations that, for a fixed amount of power demand, networks with distributed generation do better in achieving and maintaining synchronous behavior, as well as in recovering the synchronous behavior after a perturbation. To
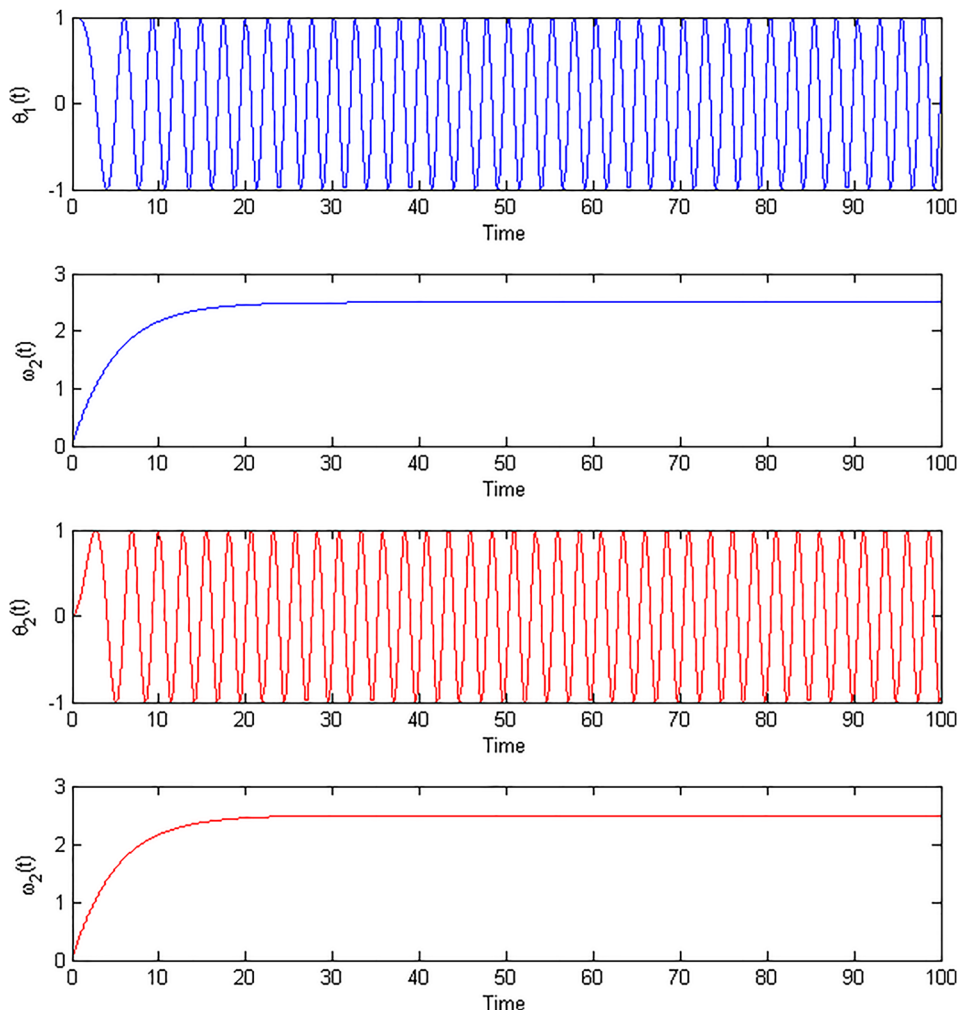

FIG. 3. Time evolution of two mutually coupled Kuramoto-like oscillators with $P_{max} = 1.5$, $P_1 = 2$, $P_2 = -1$ in a generator-motor configuration (G-M) $\omega_1(0) = \omega_2(0) = 0$. The value of the coupling strength, obtained by means of Equation (19), is the minimum for which synchronization between such oscillators can be maintained.
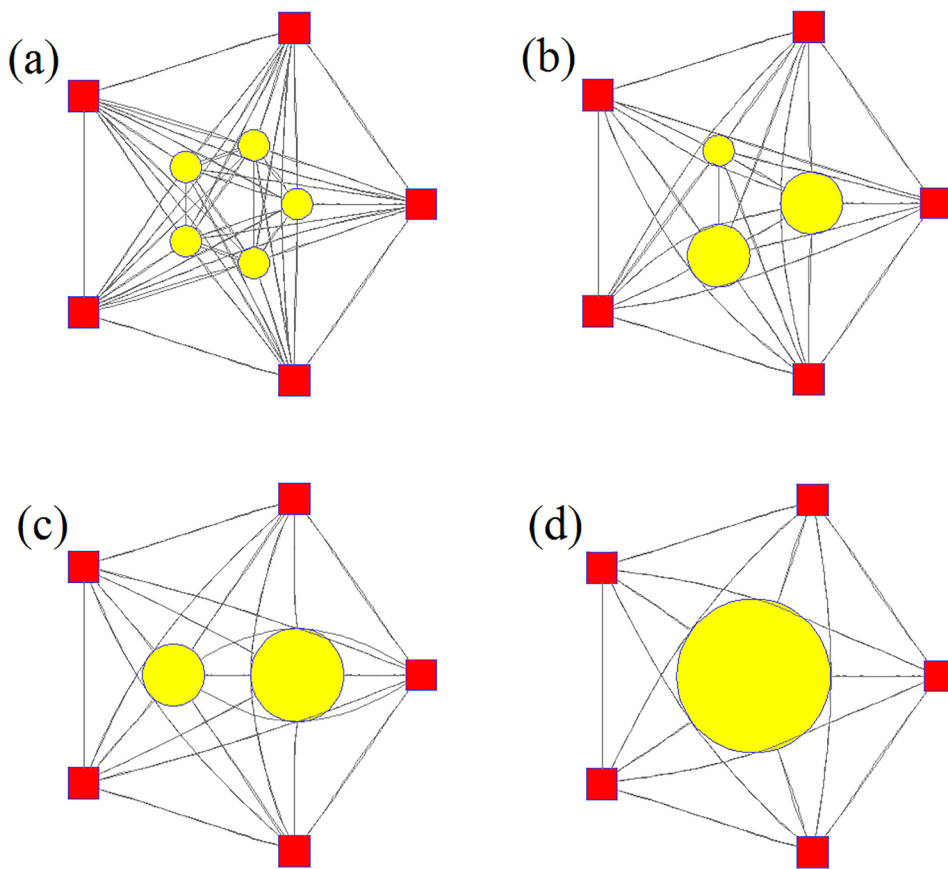
FIG. 4. (a) Network with 5 generators ($P_G = 1$ each) and 5 motors ($P_M = -1$ each). (b) Network with 3 generators ($P_{G1} = P_{G2} = 2$, $P_{G3} = 1$) and 5 motors ($P_M = -1$ each). (c) Network with 2 generators ($P_{G1} = 3$, $P_{G2} = 2$) and 5 motors ($P_M = -1$ each). (d) Network with 1 generator ($P_G = 5$) and 5 motors ($P_M = -1$ each).

illustrate this, Figure 4 shows networks with $\sum P_M = -5$ and different levels power generation architecture, from (a) the most distributed to (d) the most centralized one. Results show that both P_{max} and P_{sm} increase as the power generation becomes more centralized, which means that the conditions for stable frequency synchronization become more stringent with centralization. Parameter values for these simulations are shown in Table I.

Note that P_{max} and P_{sm} increase monotonically with the increase in $max\{P_i - P_j\}$ and in the number of nodes N, which influences E_{max}. This can be read also from Eqs. (17) and (4).

C. A tour over the $N \times \Delta P$ parameter space

A study of the behavior of P_{max} over the parameter space $N \times \Delta P$ gives a more general account of how these parameters influence synchronization. It can be noted from Figure 5 that the value of P_{max} increases more steeply along the vertical axis, labeled $max(\triangle P_{ij})$ and defined as $max(P_i - P_j)$, $i, j = 1, \ldots N$.

TABLE I. Comparison of the coupling values for the cases presented in Figure 4.

Case	$max\{P_i - P_j\}$	N	P_{sm}	P_{max}^{**}
(a)	2	10	0.111	0.181
(b)	3	8	0.286	0.396
(c)	4	7	0.500	0.655
(d)	6	6	1.000	1.249

Thus, concerning the power-grid model of second-order Kuramoto oscillators, it can be concluded that the heterogeneity of the oscillators in the network, with respect to their generated/consumed power, is more influential for the synchronizability than for the network size.

D. A real power-grid: SIN—National Interconnected System

The National Interconnected System, in Brazil, is a countrywide power system composed of 96 000 km of high-voltage transmission lines, over 1000 generation units and
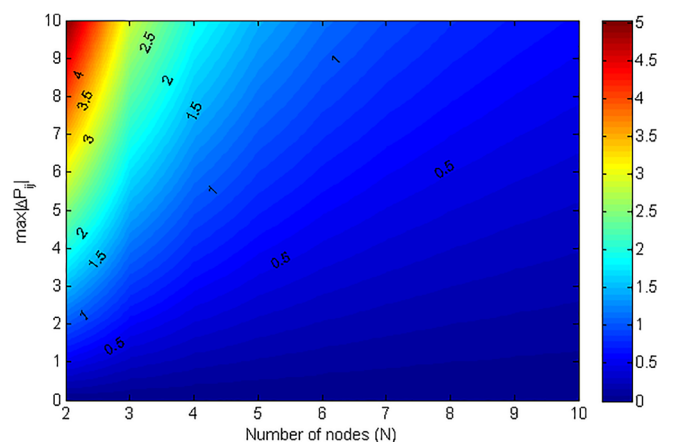

FIG. 5. Contour plot showing the evaluation of P_{max} as a function of the number of nodes in the network (N) and the maximum difference between power input/outputs, $max|\Delta P_{ij}|$.
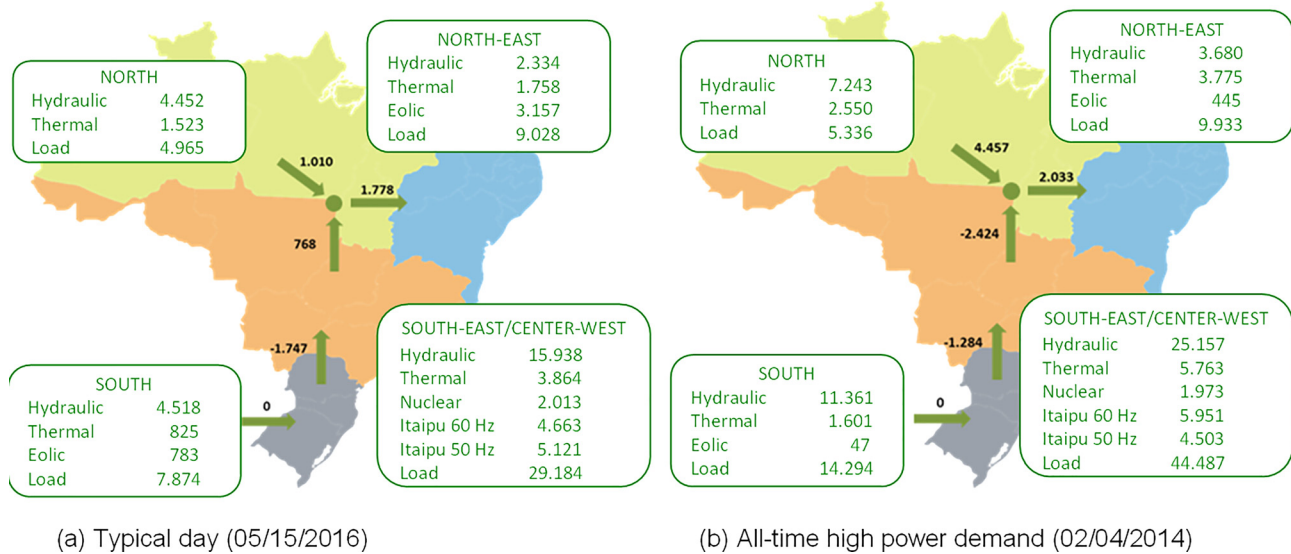
FIG. 6. Charts of generation and load: the composition of the sources include Hydro, Thermal Eolic and Nuclear generators. Mean values and direction of power transfers are informed by the arrows and associated amounts given in Gigawatts (GW). (a) Power transfers for a typical day; (b) Power transfers in the occasion of the all-time-high power demand day in which a major blackout occurred. Adapted from Ref. 31.

800 circuits.[31] Around 200 of the generating units have nominal capacities above 30 MW and the system can deliver over 130 GW. The generation includes hydro (70.8%), natural gas (10.5%), oil (4.0%), biomass (3.8%), nuclear (1.8%), and eolic (0.2%). SIN is composed by four subsystems: North (N), North-East (NE), South-East/Center-West (SE/CO), and South (S), as shown in Fig. 6. The statistics for the graph of the high-voltage generation and transmission system is presented in Table II.

In a typical day, the system operates within 30–40% of its installed capacity.[31] In other days, these figures can reach 60–70%. Figure 6 illustrates this fact: (a) load demand for a typical day and (b) load demand for a usual day when an all-time-high instantaneous demand occurred, followed by a blackout. We apply the framework developed in Section III to evaluate the requirements on P_{max} in each case. Towards this end, we consider the bulk portion of SIN transmission network, pictured in Figure 7(a). From this, one obtains a network of bulk power transfers among the 4 subsystems, as pictured in Figure 7(b). The reference values and direction of power flow for each case are given in Figure 6. Considering

that the network is composed of $N = 4$ nodes, the values of power transfers are scaled down such that the magnitude of the maximum power generation/demand for any region is $P \leq 4$ (Fig. 8).

The results of simulations under these conditions are presented in Figures 9 and 10. The results in Figure 9 indicate $P_{sm} = 0.752$ and $P_{max} = 1.176$ for the conditions presented in Figure 6(a)—typical day. These are considerably lower than those corresponding to the conditions presented in Figure 6(b)—all-time high, which are $P_{sm} = 1.333$ and $P_{max} = 1.891$. The analytical estimates for P_{max} are closely matched by the numerical results, as it can be read from Figures 9 and 10. In any case, these values indicate that, indeed, the condition under which the February 4, 2014, blackout in Brazil occurred was one of significantly large coupling strength requirement in comparison with the one that is observed in a typical day. Under these conditions, it was shown that the conditions for complete frequency locking become more stringent since the critical coupling for the onset of complete frequency locking becomes higher.

Another dynamical effect of heavier power transfers and more unbalanced generation/consumption per region can be visualized by comparing Figures 9 and 10. The simulation results show the contour plot for the order parameter r_f, defined in Equation (21), as a function of the coupling, P_{max}, the length of the shortest arc in the cycle that covers the geodesic distance between any two initial condition angles of the oscillators, γ, defined before (Fig. 11). From these pictures, it can be noted that the heavier power transfers and more unbalanced generation/consumption per region, as depicted in Figure 12, cause the phase locking region to shrink significantly. This not only causes synchronization to be more difficult to occur but also causes the network to be more likely to lose synchronization due to perturbations.

TABLE II. Statistics of the network of the National Interconnected System (SIN), in Brazil, and each of its subsystems.

Property	SIN	N	NE	CO/CO	S
Number of nodes	1.201	351	337	350	138
Number of edges	1.459	434	420	408	157
Mean degree	2.429	2.472	2.493	2.326	2.275
Max. degree	12	8	11	12	8
Clustering coefficient	0.042	0.061	0.042	0.031	0.021
Average path length	14.329	8.581	7.984	8.907	8.381
Diameter	33	23	21	20	24
Degree assortativity	−0.005	−0.047	−0.037	0.023	−0.013

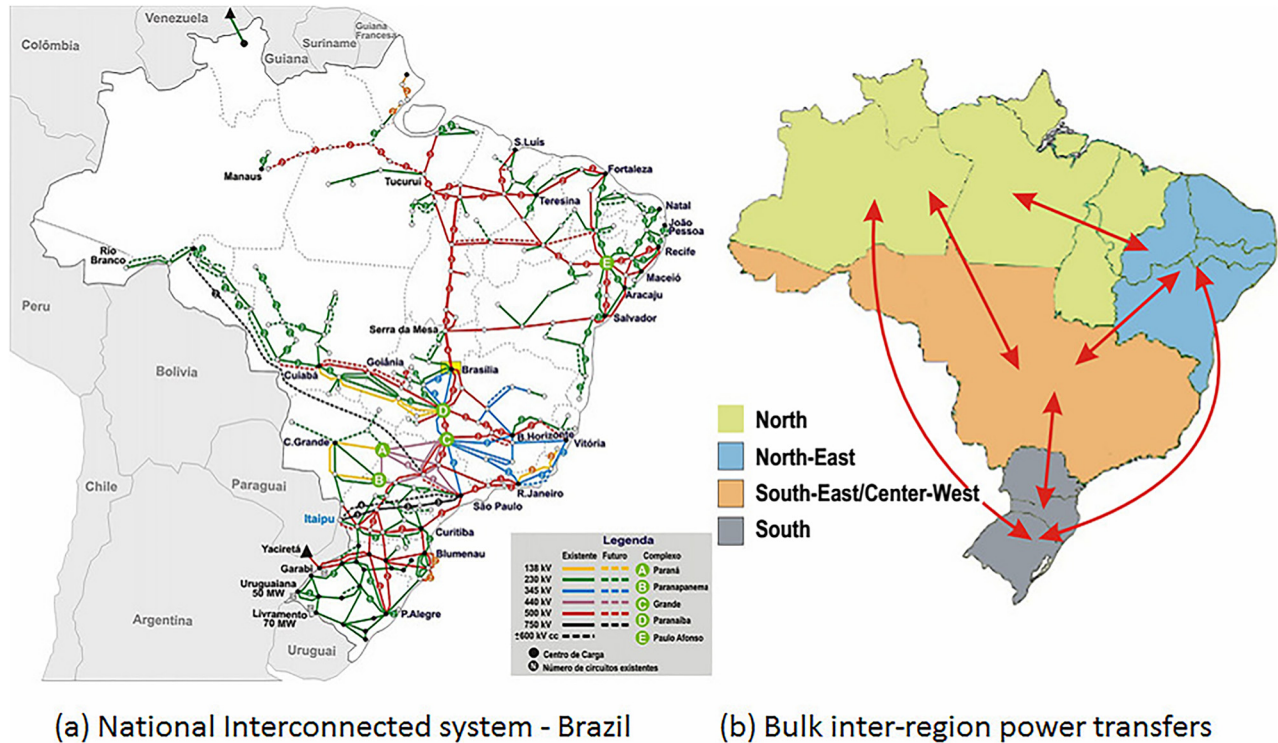(a) National Interconnected system - Brazil   (b) Bulk inter-region power transfers

FIG. 7. (a) National Interconnected System (SIN) in Brazil, the countrywide electrical power transmission system. Rated line voltages range from 138 kV to 750 kV for AC transmission and 600 kV for DC transmission. The system is sectioned into four subsystems: North (N), North-East (NE), South-East/Center-West (SE/CO) and South (S). (b) Network of the bulk inter-region power transfers. Adapted from Ref. 31.

V. DISCUSSION

Under $|P_i| \cong |P_j|$, the results developed in Section III establish less restrictive necessary condition for the emergence of synchronization. Hence, the line capacity $max(P^*_{max}, P_{sm})$ gives the minimum value of coupling for which synchronization can set in. In practice, this value affects the calculations of bus and line capacities, especially under contingency situations as power flow must be redirected in such a way that the condition $P_{max} \geq max(P^*_{max}, P_{sm})$ is still verified for the nodes and links that remain working in the post-fault condition.

Regarding the estimation of P^{**}_{max} in Equation (17), it shows that the coupling strength has to be large enough to overcome the heterogeneity of the oscillators, as expressed by $P_i - P_j$, and the difference of angular velocities, $\Delta\omega_{max}$.

This criterion agrees with previous results developed on the basis of different approaches, analytical and numerical, found in recent papers.[3,5,29] Further evidence of the consistence of the results is that they agree with numerical simulations with significant accuracy. The behavior of monotonic increase of E_{max} as $N \to \infty$, along with the direct linear dependence of P_{max} on the node heterogeneity $\Delta P = |P_i - P_j|$, suggests that larger networks with more distributed power generation, that is, $|P_i| \cong |P_j|$, can achieve and maintain synchronization more easily with respect to the coupling strength.

VI. CONCLUSIONS

This work provided some useful analytical expressions to estimate the coupling strength with a view on the onset of complete frequency locking in networks of second-order Kuramoto oscillators. Rather than assuming that the oscillators are currently synchronized in order to derive an expression for the onset of complete frequency locking, we simply observe that their angular velocities shall lie within a compact set with known boundaries and then estimate their limits. The theoretical expressions were evaluated by means of an order parameter associated with synchronization quality and persistence. Case studies were carried out to illustrate the applicability of the proposed theoretical results which were seen to closely match the data obtained by numerical simulations. Further, a case study considering the National Interconnected System shed a light on the likely factors contributing to the 2014 blackout, that is, centralized generation and heavy power flow.
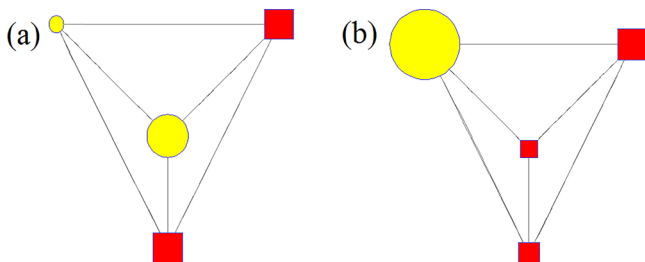

FIG. 8. Graph representation of the subsystems of SIN for each of the conditions depicted in Figure 6. (a) Network with 2 generators ($P_{G1} = 0.91$, $P_{G2} = 2.26$) and 2 motors ($P_{M1} = -1.60$, $P_{M2} = -1.57$). (b) Network with 1 generator ($P_{G1} = 4.00$) and 3 motors ($P_{M1} = -1.82$, $P_{M2} = -1.02$, $P_{M3} = -1.16$).
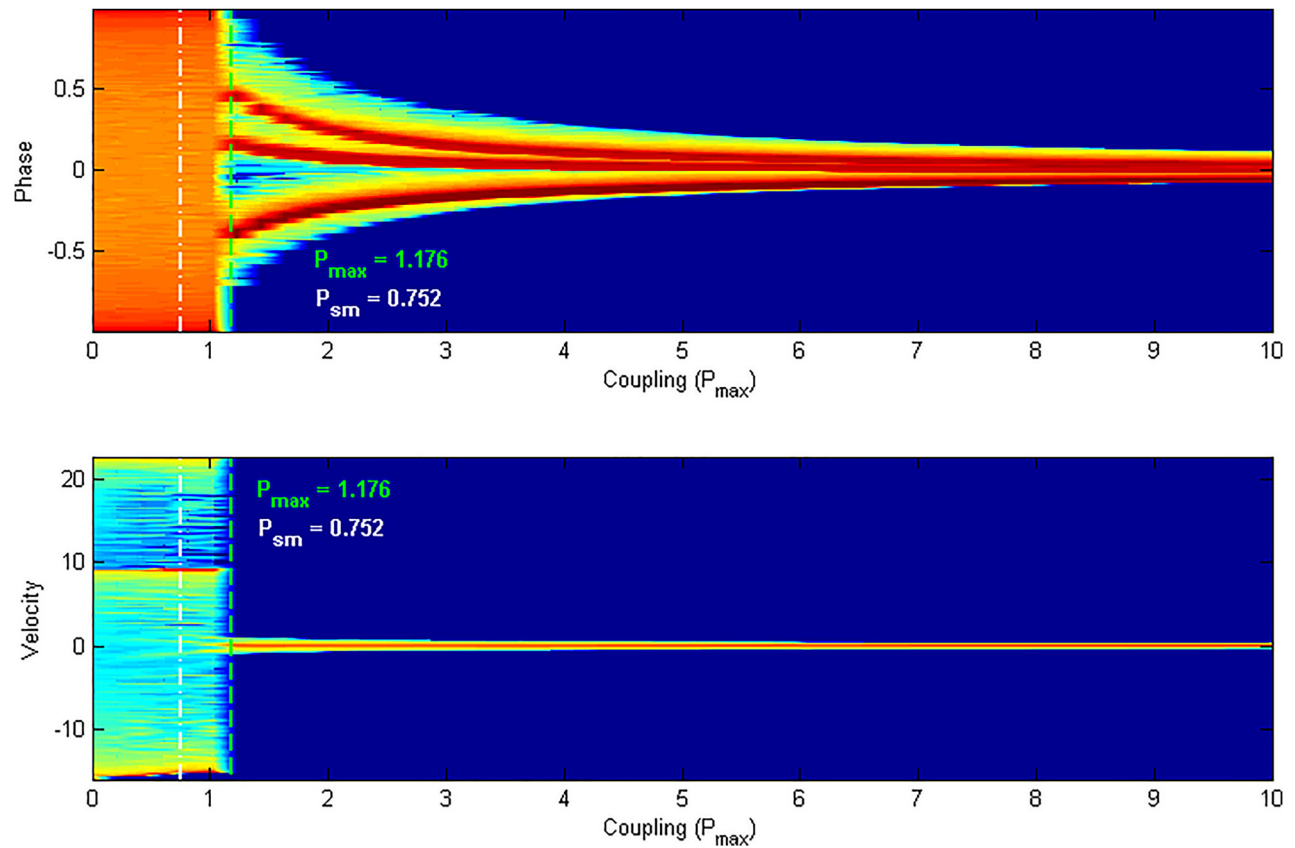
FIG. 9. Numerical simulation of the mean values of power transfers presented in Figure 6(a). The synchronization manifold exists for $P_{sm} \geq 0.752$ and synchronization sets in for $P_{max} \geq 1.176$.
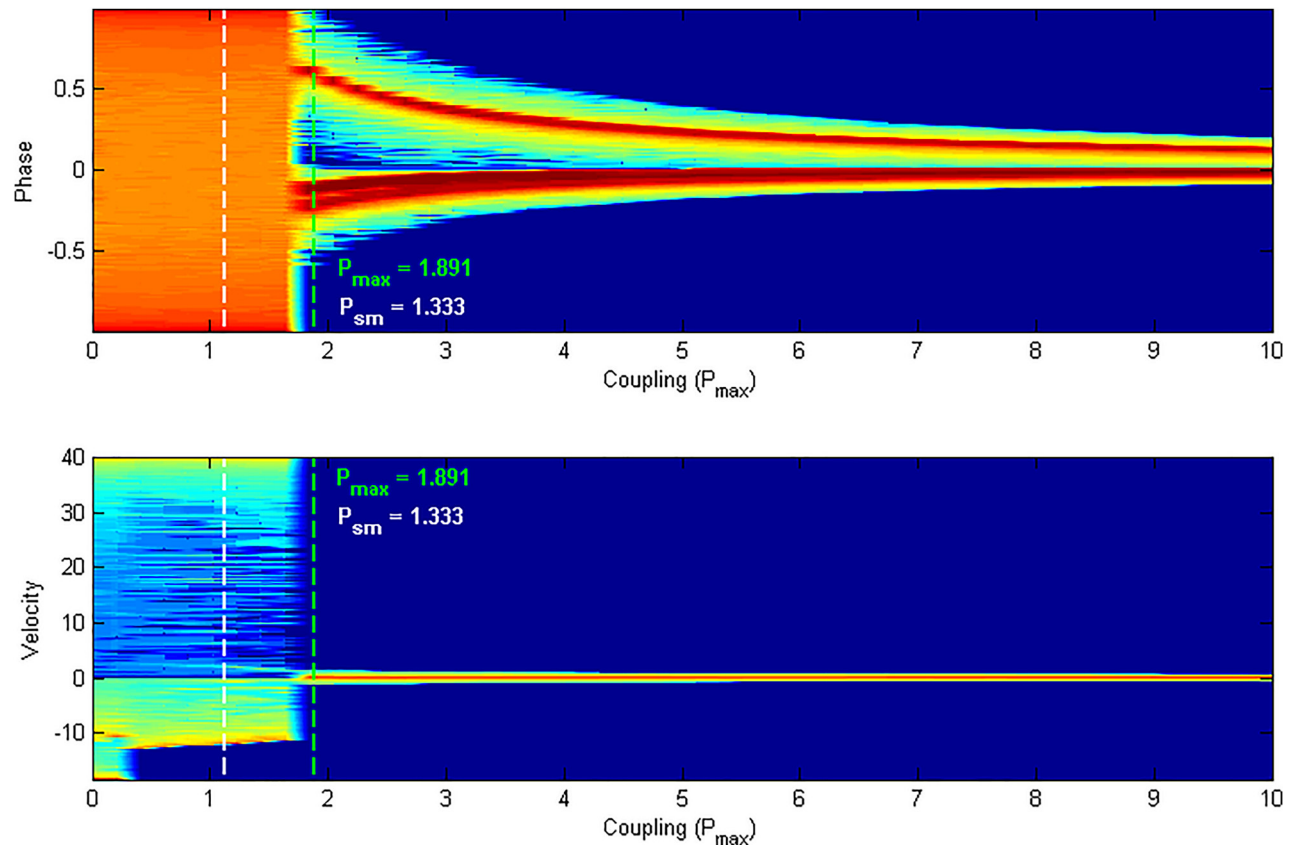

FIG. 10. Numerical simulation of the mean values of power transfers presented in Figure 6(b). The synchronization manifold exists for $P_{sm} \geq 1.333$ and synchronization sets in for $P_{max} \geq 1.891$.
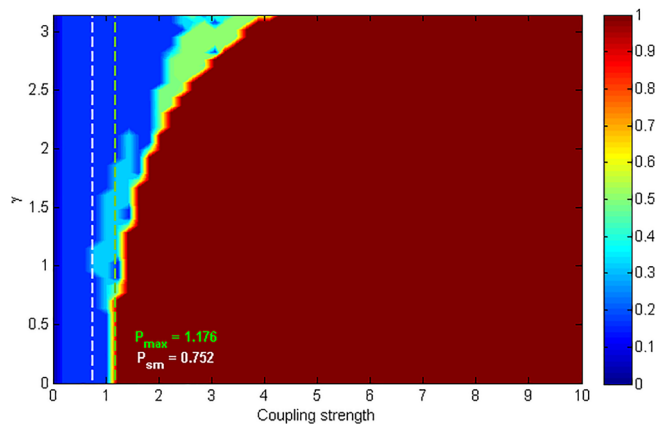
FIG. 11. Numerical simulation of the mean values of power transfers presented in Figure 6(a). The synchronization manifold exists for $P_{sm} \geq 0.752$ and synchronization sets in for $P_{max} \geq 1.176$.
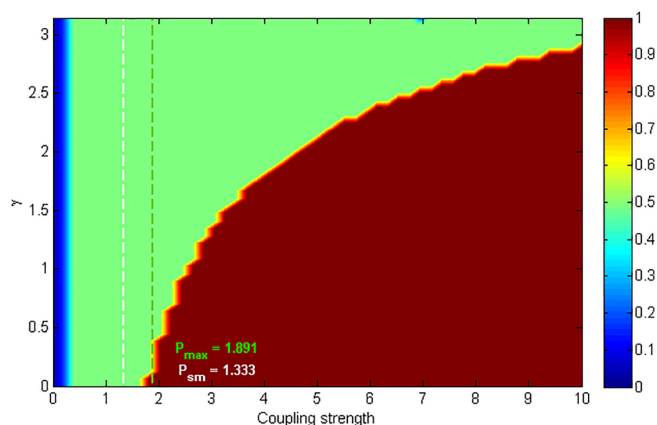

FIG. 12. Numerical simulation of the mean values of power transfers presented in Figure 6(b). The synchronization manifold exists for $P_{sm} \geq 1.333$ and synchronization sets in for $P_{max} \geq 1.891$.

ACKNOWLEDGMENTS

[1]G. Andersson, P. Donalek, R. Farmer, N. Hatziargyriou, I. Kamwa, P. Kundur, N. Martins, J. Paserba, P. Pourbeik, J. Sanchez-Gasca, R. Schulz, A. Stankovic, C. Taylor, and V. Vittal, "Causes of the 2003 major grid blackouts in North America and Europe, and recommended means to improve system dynamic performance," IEEE Trans. Power Syst. **20**(4), 1922–1928 (2005).

[2]A. Arenas, A. Diaz-Guilera, J. Kurths, Y. Moreno, and C. S. Zhou, "Synchronization in complex networks," Phys. Rep. **469**, 93–153 (2008).

[3]R. Carareto, M. S. Baptista, and C. Grebogi, "Natural synchronization in power-grids with anti-correlated units," Commun. Nonlinear Sci. Numer. Simul. **18**(4), 1035–1046 (2013).

[4]Y.-P. Choi, S.-Y. Ha, and S.-B. Yun, "Complete synchronization of Kuramoto oscillators with finite inertia," Physica D **240**(1), 32–44 (2011).

[5]Y.-P. Choi, Z. Li, S.-Y. Ha, X. Xue, and S.-B. Yun, "Complete entrainment of Kuramoto oscillators with inertia on networks via gradient-like flow," J. Differ. Equations **257**(7), 2591–2621 (2014).

[6]N. Chopra and M. W. Spong, "On synchronization of Kuramoto oscillators," in Proceedings of the 44th IEEE Conference on Decision and Control and the European Control Conference, Seville, Spain, 12–15 December 2005, pp. 3916–3922.

[7]S. Corsi and C. Sabelli, "General blackout in Italy Sunday September 28, 2003, h. 03:28:00," in IEEE Power Engineering Society General Meeting (2004), pp. 1691–1702.

[8]P. Crucitti, V. Latora, and M. Marchiori, "Model for cascading failures in complex networks," Phys. Rev. E **69**, 045104 (2004).

[9]P. Crucitti, V. Latora, and M. Marchiori, "A topological analysis of the Italian electric power grid," Physica A **338**, 92–97 (2004).

[10]P. Crucitti, V. Latora, M. Marchiori, and A. Rapisarda, "Error and attack tolerance of complex networks," Physica A **340**, 388–394 (2004).

[11]D. Cumin and C. P. Unsworth, "Generalising the kuramoto model for the study of neuronal synchronisation in the brain," Physica D **226**(2), 181–196 (2007).

[12]F. Dorfler and F. Bullo, "Synchronization and transient stability in power networks and non-uniform kuramoto oscillators," SIAM J. Control Optim. **50**, 1616 (2010).

[13]F. Dorfler and F. Bullo, "Synchronization in complex networks of phase oscillators: A survey," Automatica **50**(6), 1539–1564 (2014).

[14]F. A. S. Ferrari, R. L. Viana, S. R. Lopes, and R. Stoop, "Phase synchronization of coupled bursting neurons and the generalized kuramoto model," Neural Networks **66**, 107–118 (2015).

[15]G. Filatrella, A. H. Nielsen, and N. F. Pedersen, "Analysis of a power grid using a Kuramoto-like model," Eur. Phys. J. B **61**, 485–491 (2008).

[16]Union for the Coordination of Electricity Transmission (UCTE), Final Report of the Investigation Committee on the 28 September 2003 Blackout in Italy, 2004.

[17]US-Canada Power System Outage Task Force, Final Report on the August 14, 2003 blackout in the United States and Canada, 2004.

[18]L. Fortuna, M. Frasca, and A. S. Fiore, "Analysis of the Italian power grid based on kuramoto-like model," Physcon 2011, Leon, Spain, 5–8 September 2008.

[19]A. Franci, A. Chaillet, and W. Pasillas-Lépine, "Existence and robustness of phase-locking in coupled kuramoto oscillators under mean-field feedback," Automatica **47**(6), 1193–1202 (2011).

[20]J. Gomes-Gardenes, Y. Moreno, and A. Arenas, "Paths to synchronization on complex networks," Phys. Rev. Lett. **98**, 034101 (2007).

[21]P. Hines, S. Blumsack, E. C. Sanchez, and C. Barrows, "The topological and electrical structure of power grids," 43rd Hawaii International Conference on System Sciences (HICSS), 5–8 January 2010.

[22]I. Kashchenko and S. Kaschenko, "Dynamics of the Kuramoto equation with spatially distributed control," Commun. Nonlinear Sci. Numer. Simul. **34**, 123–129 (2016).

[23]P. Kundur, Power System Stability and Control (McGraw-Hill, 1994).

[24]H. Lee Willis, Power Distribution Planning Reference Book (Marcel Dikker, Inc., 2004).

[25]P. J. Menck, J. Heitzig, J. Kurths, and H. J. Schellnhuber, "How dead ends undermine power grid stability," Nat. Commun. **5**, 3969 (2014).

[26]P. J. Menck, J. Heitzig, N. Marwan, and J. Kurths, "How basin stability complements the linear-stability paradigm," Nat. Phys. **9**, 89–92 (2013).

[27]R. E. Mirollo and S. H. Strogatz, "The spectrum of the locked state for the Kuramoto model of coupled oscillators," Physica D **205**(1–4), 249–266 (2005).

[28]A. E. Motter, S. A. Myers, M. Anghel, and T. Nishikawa, "Spontaneous synchrony in power-grid networks," Nat. Phys. **9**, 191–197 (2013).

[29]S. Olmi, A. Navas, S. Boccaletti, and A. Torcini, "Hysteretic transitions in the Kuramoto model with inertia," Phys. Rev. E **90**, 042905 (2014).

[30]ONS, Operador nacional do sistema eletrico, Indicadores de continuidade dos pontos de controle da rede basica, 2014.

[31]ONS, Operador nacional do sistema eletrico, Analise da carga de energia e demanda, Boletim de carga, 2016.

[32]R. S. Pinto and A. Saa, "Synchrony-optimized networks of Kuramoto oscillators with inertia," Physica A **463**, 77–87 (2016).

[33]F. A. Rodrigues, T. K. DM. Peron, P. Ji, and J. Kurths, "The Kuramoto model in complex networks," Phys. Rep. **610**, 1–98 (2016).

[34]M. Rohden, A. Sorge, M. Timme, and D. Witthaut, "Self-organized synchronization in decentralized power grids," Phys. Rev. Lett. **109**, 064101 (2012).

[35]M. Rosas-Casals, S. Valverde, and R. V. Sole, "Topological vulnerability of the European power grid under errors and attacks," Int. J. Bifurcation Chaos **17**, 2465–2475 (2007).

[36]K. Schmietendorf, J. Peinke, R. Friedrich, and O. Kamps, "Self-organized synchronization and voltage stability in networks of synchronous machines," Eur. Phys. J. Spec. Top. **223**(12), 2577–2592 (2014).

[37]P. Schultz, J. Heitzig, and J. Kurths, "Detours around basin stability in power networks," New J. Phys. **16**, 125001 (2014).

[38]R. V. Solé, M. Rosas-Casals, B. Corominas-Murtra, and S. Valverde, "Robustness of the European power grids under intentional attack," Phys. Rev. E **77**, 026102 (2008).

[39]S. H. Strogatz, "From Kuramoto to Crawford: Exploring the onset of synchronization in populations of coupled oscillators," Physica D **143**(1–4), 1–20 (2000).

[40]Y. Susuki, I. Mezić, and T. Hikihara, "Coherent swing instability of power grids," J. Nonlinear Sci. **21**(3), 403–439 (2011).

[41]H.-A. Tanaka, A. J. Lichtenberg, and S. Oishi, "First order phase transition resulting from finite inertia in coupled oscillator systems," Phys. Rev. Lett. **78**, 2104–2107 (1997).

[42]K. Wiesenfeld, P. Colet, and S. H. Strogatz, "Synchronization transitions in a disordered Josephson series array," Phys. Rev. Lett. **76**, 404–407 (1996).